

| REPORT DOCUMENTATION PAGE | | | | Form Approved OMB No. 0704-0188 | |
|--|-----------------------------|------------------------------------|--|---|--|
| <small>Public reporting burden for this collection of information is estimated to average 1 hour per response, including the time for reviewing instructions, searching existing data sources, gathering and maintaining the data needed, and completing and reviewing this collection of information. Send comments regarding this burden estimate or any other aspect of this collection of information, including suggestions for reducing this burden to Department of Defense, Washington Headquarters Services, Directorate for Information Operations and Reports (0704-0188), 1215 Jefferson Davis Highway, Suite 1204, Arlington, VA 22202-4302. Respondents should be aware that notwithstanding any other provision of law, no person shall be subject to any penalty for failing to comply with a collection of information if it does not display a currently valid OMB control number. PLEASE DO NOT RETURN YOUR FORM TO THE ABOVE ADDRESS.</small> | | | | | |
| 1. REPORT DATE (DD-MM-YYYY) August 2012 | | 2. REPORT TYPE Conference Paper | | 3. DATES COVERED (From - To) | |
| 4. TITLE AND SUBTITLE Split Stream Flow Past a Blunt Trailing Edge with Application to Combustion Instabilities | | | | 5a. CONTRACT NUMBER | |
| | | | | 5b. GRANT NUMBER | |
| | | | | 5c. PROGRAM ELEMENT NUMBER | |
| 6. AUTHOR(S) Vicky Tian, Beverley McKeon, Ivett A Leyva | | | | 5d. PROJECT NUMBER | |
| | | | | 5e. TASK NUMBER | |
| | | | | 5f. WORK UNIT NUMBER Q0AY/23080533 | |
| 7. PERFORMING ORGANIZATION NAME(S) AND ADDRESS(ES) AFRL/RQRC 10 E. Saturn Blvd. Edwards AFB CA 93524-7680 | | | | 8. PERFORMING ORGANIZATION REPORT NO. | |
| 9. SPONSORING / MONITORING AGENCY NAME(S) AND ADDRESS(ES) Air Force Research Laboratory (AFMC) AFRL/RQR 5 Pollux Drive Edwards AFB CA 93524-7048 | | | | 10. SPONSOR/MONITOR'S ACRONYM(S) | |
| | | | | 11. SPONSOR/MONITOR'S REPORT NUMBER(S) AFRL-RQ-ED-TP-2012-249 | |
| 12. DISTRIBUTION / AVAILABILITY STATEMENT Distribution A: Approved for public release; distribution unlimited. PA#12600. | | | | | |
| 13. SUPPLEMENTARY NOTES To be presented at AIAA Joint Propulsion Conference, Atlanta, GA, 29 July 2012 – 1 August 2012. | | | | | |
| 14. ABSTRACT In shear coaxial injectors, commonly used for cryogenic liquid rocket engines, propellants traveling at different velocities are separated by the inner jet post before they come into contact with each other, mix, and combust. Knowing how the fluids mix and how susceptible they are to hydrodynamic instabilities is paramount for a successful liquid rocket engine. In this study, the wake behind a blunt trailing edge of a long plate, similar to an unwrapped coaxial injector, was studied in a water tunnel. Two fluid streams of different velocities were introduced on opposite sides of the plate. PIV was used to visualize and determine the influence of the velocity ratio of the split stream on the wake behavior. Measurements of the vortex shedding frequency were taken at various velocity ratios and compared with well characterized cases with a uniform free stream. Operating conditions ranged from Reynolds number 6,000 to 22,000 and velocity ratios 0.30 to 1.00. | | | | | |
| 15. SUBJECT TERMS | | | | | |
| 16. SECURITY CLASSIFICATION OF: | | | 17. LIMITATION OF ABSTRACT SAR | 18. NUMBER OF PAGES 14 | 19a. NAME OF RESPONSIBLE PERSON Douglas Talley |
| a. REPORT Unclassified | b. ABSTRACT Unclassified | c. THIS PAGE Unclassified | | | 19b. TELEPHONE NO (include area code) N/A |

Split Stream Flow Past a Blunt Trailing Edge with Application to Combustion Instabilities

Vicky Tian¹, Beverley McKeon²

California Institute of Technology, Pasadena, CA 91125, USA

Ivett A Leyva³

Air Force Research Lab, Edwards AFB, CA 93524, USA

In shear coaxial injectors, commonly used for cryogenic liquid rocket engines, propellants traveling at different velocities are separated by the inner jet post before they come into contact with each other, mix, and combust. Knowing how the fluids mix and how susceptible they are to hydrodynamic instabilities is paramount for a successful liquid rocket engine. In this study, the wake behind a blunt trailing edge of a long plate, similar to an unwrapped coaxial injector, was studied in a water tunnel. Two fluid streams of different velocities were introduced on opposite sides of the plate. PIV was used to visualize and determine the influence of the velocity ratio of the split stream on the wake behavior. Measurements of the vortex shedding frequency were taken at various velocity ratios and compared with well characterized cases with a uniform free stream. Operating conditions ranged from Reynolds number 6,000 to 22,000 and velocity ratios 0.30 to 1.00.

Nomenclature

| | | |
|-------------------|---|--|
| t | = | plate thickness [m] |
| U_1 | = | mean free stream velocity of faster, unobstructed stream [m s^{-1}] |
| U_2 | = | mean free stream velocity of slower, obstructed stream [m s^{-1}] |
| ρ | = | density of fluid [N s m^{-2}] |
| μ | = | dynamic viscosity [kg m^{-2}] |
| f | = | shedding frequency of vortices from one stream [Hz] |
| U_{mean} | = | $\frac{1}{2} (U_1 + U_2)$ mean of two free streams [m s^{-1}] |
| VR | = | U_1/U_2 velocity ratio |
| Re | = | Reynolds number using U_{mean} |
| St | = | $f t/U$ - Strouhal number using U_{mean} |

I. Introduction

SHEAR coaxial injectors are a common choice for cryogenic liquid rocket engines such as the Shuttle SSME or the Delta IV booster, RS-68. In principle, the injector design is simple. There is an inner tube, carrying liquid oxygen, surrounded by a higher speed stream of hydrogen which flows through a concentric outer tube. As seen in Fig. 1, the propellants are separated by the inner jet post before they come into contact with each other, mix, and combust. This type of injector relies on the shear or difference in velocities between the two propellants to achieve good mixing. Therefore, outer to inner jet velocity ratios of the order of 10 or more are typical. When the two fluids are brought together at the end of the inner jet post, the flow is susceptible to hydrodynamic instabilities. The characteristics of a wake behind a cylinder or a blunt body have been widely characterized for the case of a single stream. However, for the case of a split stream with different velocities, there is little knowledge about how the velocity ratio affects the wake structures and shedding frequency.

¹ Undergraduate Student, AIAA Undergraduate Student Member

² Professor of Aeronautics, AIAA Senior Member.

³ Sr. Aerospace Engineer, AFRL.RZSA. AIAA Senior Member

In this project a shear coaxial injector is simplified into a basic split stream flow over a blunt trailing edge (Fig. 2). This can be thought of as an “unwrapped” coaxial injector. This simplification was made for ease of visualization and measurements. A good characterization of hydrodynamic instabilities for the case of non-reacting flows is the first step to understand how combustion and heat addition will affect such instabilities. It is expected that avoiding resonances between combustion processes and hydrodynamic instabilities results in more stable injector designs.

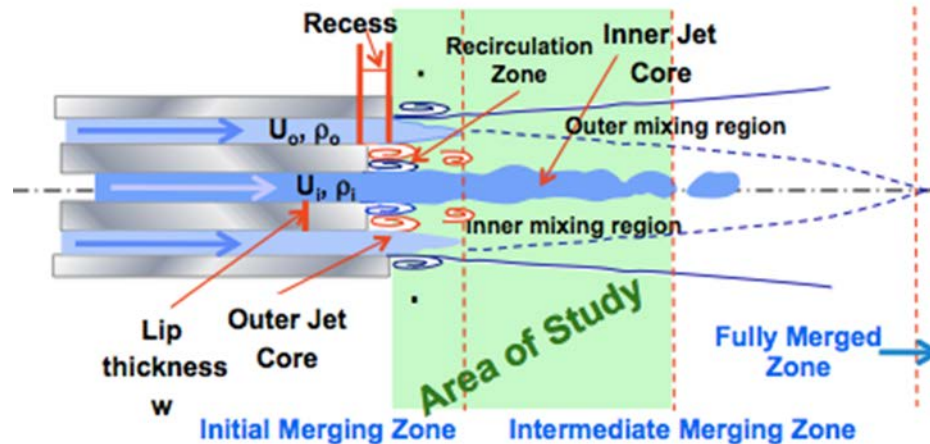


Figure 1. Schematic of shear coaxial injector relevant parameters and features.

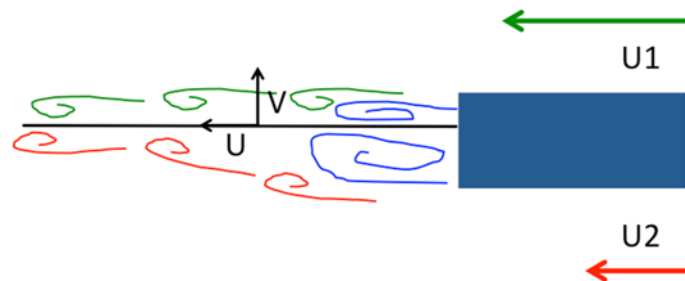


Figure 2. Simplification of shear coaxial jet used in this study.

Few investigators have documented the influence of a split stream flow around a trailing edge using hot wire measurements^{1,2,3,5,6,8}. In the case of flows with a split stream of different velocities, the wake dominates the mixing layer for some distance until the wake structures dissipate and the asymptotic turbulence structures of the mixing layer dominate. The effect of the velocity ratio has been studied mostly as it relates to the mixing layer and not the wake region and its characteristic shedding frequency. Boldman et al., using an air wind tunnel and hot wire measurements, concluded that the average velocity should be used in computing the normalized frequency or Strouhal number⁶. Using four different velocity ratios, their results showed the frequency slightly decreased as the velocity ratio was reduced. The corresponding Strouhal numbers slightly decreased then increased as velocity ratio was reduced. However, studying the Strouhal number was not the focus of his study, and he did not make concluding comments about the trend. Tamura et al. having a similar set-up, had similar results using five velocity ratios⁸. They concluded that the Strouhal numbers for velocity ratios greater than 0.78 can be approximated by the Strouhal numbers of the uniform case. Their data also showed that below ratio 0.78, the Strouhal numbers decreased then increased from the uniform case. However, he did not comment on the results for ratios lower than 0.78.

Flows that present a combination of wake and shear layer phenomena are also very interesting from the point of view of linear stability analysis. For example, wakes are a well-known example of absolutely unstable flows whereas shear layers are a classical example of convectively unstable flows. Wallace and Redekopp⁹, in a computational study, map the stability characteristics (convective vs. absolutely unstable) for plane wake-shear layer

as a function of two parameters, a wake deficit parameter (velocity deficit divided by the mean velocity) and a velocity ratio (the velocity difference across the layer of nonzero vorticity divided by the mean velocity). They predict that downstream of the wake region, the vortex pattern should transition into a single row of vortex structures. Bocanegra-Evans and Allen¹⁰ confirmed experimentally those predictions showing that for certain velocity ratios, for the case of a splitter plate with a cylinder at the end, the flow has first a strong Von-Karman street mode which transitions to a single vortex rollup characteristic of shear layers. The single shear layer structures are seen in the high speed side of the flow. Finally, more recently Laizet et al.¹¹ using DNS studied the effect of the end geometry of the splitter plate (blunt, sharp beveled, truncated bevel) on the flow development. They also showed that for the case of a blunt edge, the wake gives way to a single vortex structure characteristic of shear layers.

The main objective of this study is to characterize the dependence of the hydrodynamic instabilities developed downstream of a blunt edge on the velocity ratio and Reynolds number between the two incoming streams. Particle Image Velocimetry (PIV) is used to visualize the flow field and measure the stream velocities and frequencies. Hotwire techniques can only measure velocity at a single point whereas PIV can measure velocity in a plane, thus providing a clearer picture of the structures in the wake.

II. Experimental Set up and Procedure

A. Apparatus

Tests were carried out in the NOAH water tunnel at the Graduate Aerospace Laboratories of California Institute of Technology. The experimental set up consisted of an upstream dividing plate 0.057m thick and 3.5m long. It was placed vertically in the water tunnel. Due to its length, the plate was constructed in three sections: two 1.5m long wooden planks treated with water-resistant paint and one 0.5m long acrylic hollow plate with a blunt trailing edge. The wood was placed upstream and the acrylic downstream, to give optical access through the plate at the location of the subsequent PIV measurements.

B. Variation of Velocity Ratio

The velocities of each stream in the water tunnel were controlled using honeycomb, wire mesh, and cloth. The plastic honeycomb had cells 1/8-inches in diameter, and blocks of the honeycomb approximately 1-inch and 2-inch thick were used. The wire mesh had a square mesh approximately 1/16-inches in width. The types of cloths used were loosely woven cotton cheesecloth, a slightly denser muslin cheesecloth, and polyester filter felt.

To vary the velocity ratio, honeycomb, mesh, and cloth were introduced to one side of the plate while the other velocity remained unchanged. They were placed as far upstream as possible; in this case, at the start of the wooden plate. Because the velocity was not completely uniform across the flow due to boundary layers forming on the plate and walls, free stream velocity of each flow (U_1 and U_2) was taken as the time-average velocity measured in the stream.

The following combinations were used to make the resulting velocity ratios:

- 1) 2" honeycomb
VR: 1.00-0.93
- 2) 2" honeycomb, 4 1" honeycomb, 3 screens, 2 muslin cloth
VR: 0.57-0.46
- 3) 2" honeycomb, 4 1" honeycomb, 7 screens, 5 muslin cloth, 1 filter cloth
VR: 0.32-0.30

The Reynolds number was calculated with the properties of water at room temperature and the average velocity of the two streams. The shedding frequency was non-dimensionalized using a Strouhal number ($f t/U_{\text{mean}}$) with the shedding frequency of one stream (f) as frequency, the plate thickness (t) as the length scale and the average velocity (U_{mean}) as the relevant velocity following Boldman⁶.

C. Particle Image Velocimetry (PIV)

A LaVision PIV system with and a Photonics DM20-527 solid-state laser was used to visualize the flow field, and measure the shedding frequencies and stream velocities. The PIV system used two high-speed Photron Fastcam APX-RS cameras mounted below the tunnel and a laser plane emitted from the side of the tunnel across the stream (Fig. 3). The plane was parallel to the flow aimed at the center height of the trailing edge. The sampling frequency was calculated based on the average velocity U_{mean} .

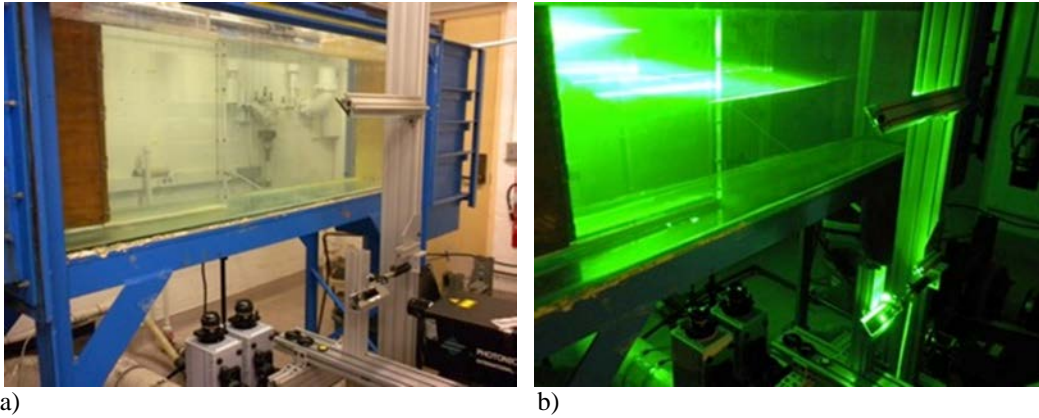


Figure 3. a) PIV Set up. b) PIV running.

D. Operating Conditions

The experiments presented here closely studied the effect of velocity ratio over three different Reynolds numbers. The specific running conditions are given in Table 1. Each Reynolds number had a base case with a velocity ratio at or close to 1.00. These base cases were used to compare the shedding frequency to the known shedding frequency of non-split stream flows. A goal of this research was to find the trend between the changing velocity ratio and Strouhal number.

Table 1. Running Conditions.

| Re | VR | Re | VR | Re | VR |
|------|------|--------|------|--------|------|
| 6196 | 0.93 | 15,185 | 0.98 | 21,430 | 1.00 |
| 6031 | 0.46 | 15,676 | 0.57 | 22,120 | 0.55 |
| 6043 | 0.30 | 14,810 | 0.32 | 21,020 | 0.32 |

III. Results

A. Time Averaged Velocity

Fig. 4-15 present time-averaged U_{mean} , V_{mean} , U_{rms} , and V_{rms} for all nine cases studied.

B. Fourier Transform Analysis

The power spectral density (PSD) of the velocity fluctuations was estimated using the Welch method of spectral estimation. Picking strategic locations in the stream allowed the shedding frequency to be picked out as the strongest peak in the power spectrum (Fig. 16).

Looking at time-instantaneous contour plots the V component, span-wise flow, of velocity, vortices can be seen with alternating positive (red) and negative (blue) V components (Fig. 17).

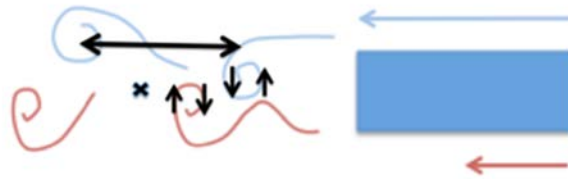


Figure 16. Shedding frequency schematic. *The upward and downward facing arrows show the v-component flow direction of certain points on the vortex.*

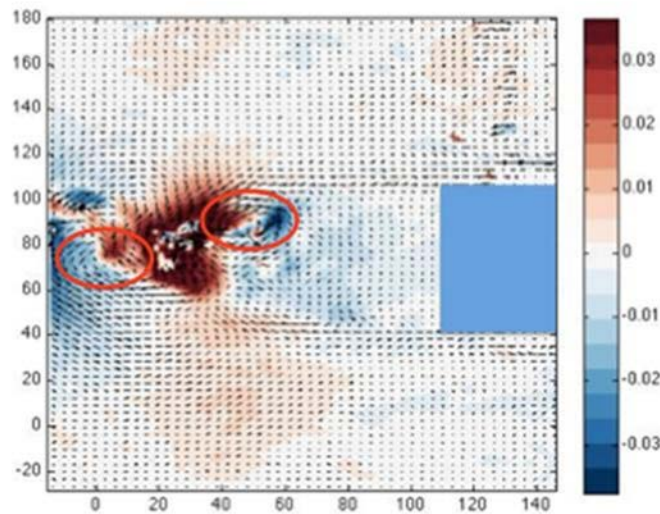


Figure 17. Example of vortices with v-component contours.

Picking points on the centerline of mixing, Fourier analysis was done on each point to find the frequency with the highest power density (Fig. 18-20). The Fourier transform analysis was done on a few points on the center of mixing line where the contour lines are very close together. Selecting points along the center of mixing line gave the strongest signal for the shedding frequency. As a general observation, the shedding frequency was consistent along the center of mixing, regardless of distance from the trailing edge, excluding the area of recirculation. This can be seen in Fig. 18-20, in which power spectra along the mixing line peaked at the same frequency. Therefore, the same dominant frequency was measured at each point along the mixing line. The mixing line shifts, moving towards the faster free stream flow, as the velocity ratio increases. This can be seen in Fig. 4-6 and Fig. 10-12.

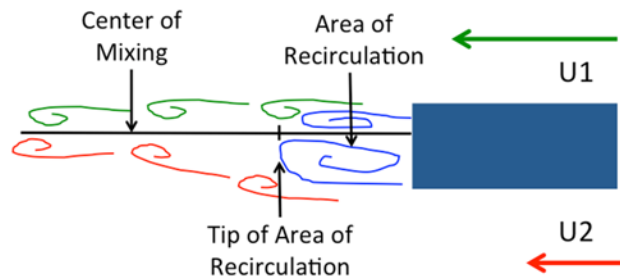


Figure 21. Schematic showing key components.

IV. Discussion

Looking at the U_{mean} and V_{mean} contour plots, we see many trends consistent with previous literature and trends that were unexpected. At the uniform, moderate, and extreme velocity ratio, with increasing Reynolds number, the area of recirculation shortens. This is expected from literature. Also, with increasing Reynolds number, the two rotating vortices in the area of recirculation become more defined. This is indicated by larger color contrasts in the contour plots. Observed only at moderate and extreme velocity ratios, the center of mixing is skewed towards the faster stream. As the velocity ratio decreases, the skew becomes more prominent. This phenomenon was not mentioned by any previous literature of similar experiments.

As velocity ratio increases with constant Reynolds number, the length of the area of recirculation seems uncorrelated. There is no linear relation to model the length of the area of recirculation. However, it can be noted that in all Reynolds number, the uniform cases have the shortest and smallest area of recirculation

The lower velocity ratios gave power spectra with multiple peaks. This may be due to the flow behind the trailing edge transitioning from a wake to a mixing layer. In a mixing layer, there is no clear shedding frequency; therefore, the lack of a clear singular shedding frequency in this experiment may be explained by this phenomenon.

Table 2. Calculated Strouhal Numbers.

| Re | VR | St | Re | VR | St | Re | VR | St |
|------|------|-------------|--------|------|-------|--------|------|-------|
| 6196 | 0.93 | 0.224 | 15,185 | 0.98 | 0.235 | 21,430 | 1.00 | 0.228 |
| 6031 | 0.46 | 0.237 | 15,676 | 0.57 | 0.250 | 22,120 | 0.55 | 0.292 |
| 6043 | 0.30 | 0.275/0.402 | 14,810 | 0.32 | 0.295 | 21,020 | 0.32 | 0.307 |

Calculating the shedding frequency and Strouhal number was the main objective. In the uniform flow case, previous literature has shown the Strouhal number has been shown to be independent of Reynolds numbers in the range of 5,000 to 20,000². Boldman shows that, independent of Reynolds number, the Strouhal number of flow around a blunt trailing edge is 0.20¹. The PSD method shows very similar measurements in the uniform case. Therefore, it can be concluded that the PSD method is valid for measuring Strouhal number. A generalization of the relationship between velocity ratio and calculated Strouhal number can be seen in Fig. 22.

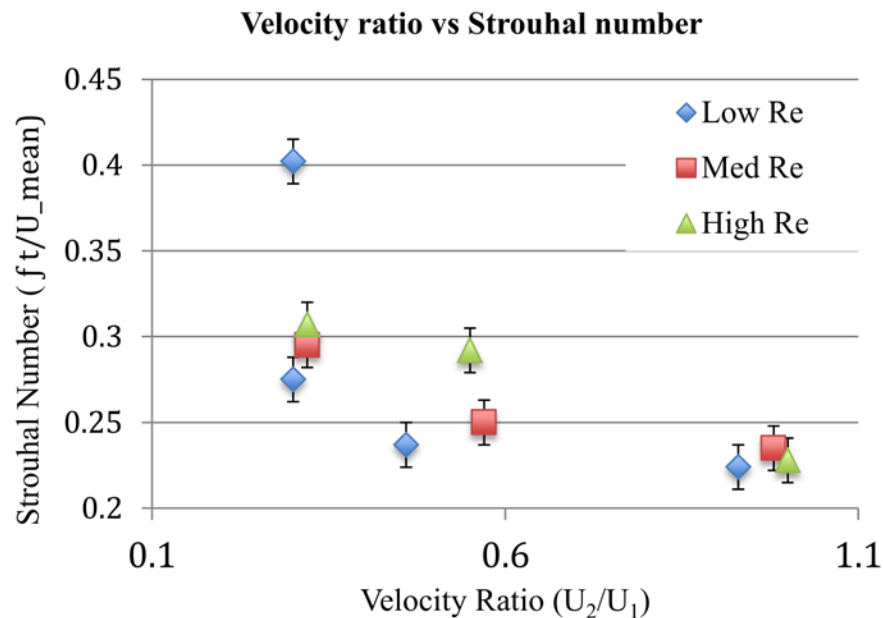


Figure 22. Velocity Ratio vs. Strouhal number. Take note that the low Re produced two equally tall peaks on the PSD at the extreme velocity ratio. Therefore, this plot shows two Strouhal numbers for the low Re, extreme VR case.

At constant Reynolds number and decreasing velocity ratio, the following changes are observed in the Strouhal number:

- Low Re: $St = (0.224, 0.237, 0.275)$ increase of 22.8%
- Med Re: $St = (0.235, 0.250, 0.295)$ increase of 25.5%
- High Re: $St = (0.228, 0.292, 0.307)$ increase of 34.7%

At constant velocity ratio and increasing Reynolds number, the following changes are observed in Strouhal number:

- Uniform VR: $St = (0.224, 0.235, 0.228)$ fluctuation of 4.9%, no linear correlated with Re
- Moderate VR: $St = (0.237, 0.250, 0.292)$ increase of 23.2%
- Extreme VR: $St = (0.275/0.402, 0.295, 0.307)$ increase of 11.6%, excluding the possible outlier 0.402

V. Conclusions

An experimental study was performed to find the dependence of Strouhal number (St) with velocity ratio for a split stream flow past a blunt trailing edge. The Strouhal number was defined using the split stream mean velocity (from previous literature) and the thickness of the trailing edge as the length scale. Three Reynolds numbers ($=\rho U_{\text{mean}}/\mu$) were studied. The experiments were conducted in a water tunnel. The primary diagnostic method was PIV.

A decrease of St by about 35% with increasing velocity ratio for three different Reynolds numbers was measured.

It was also observed that with increasing Reynolds number the area of recirculation shortens, which agrees with previous literature. Also, with increasing Reynolds number, the two rotating vortices in the area of recirculation become more defined. As the velocity ratio increases, the center of mixing is skewed towards the faster stream. As the velocity ratio decreases, the skew becomes more prominent. This phenomenon was not mentioned by any previous literature of similar experiments.

As velocity ratio increases with constant Reynolds numbers, the length of the area of recirculation seems uncorrelated. However, it can be noted that in all Reynolds numbers, the uniform cases have the shortest and smallest area of recirculation

A changing frequency with velocity ratio means a rocket design must account for several shedding frequencies, since matching between a natural frequency and a chamber acoustic frequency could lead to amplification of pressure and heat transfer oscillations.

Acknowledgments

The assistance of the Mechanical Engineering Shop at Caltech and undergraduate and graduate students of Caltech is gratefully acknowledged. The work was supported by the Air Force Research Laboratory, Lester Lees Aeronautics SURF Fellowship, Student Faculty Programs at Caltech, and Graduate Aerospace Laboratories at Caltech.

References

- ¹Boldman, D.R., Brinidh, P.F., and Goldstein, M.E., "Vortex Shedding from a Blunt Trailing Edge with Equal and Unequal External Mean Velocities," *Journal of Fluid Mechanics*, Vol. 75, No. 4, 1976, pp. 721-735
- ²Buresti, G., Talamelli, A., and Petagna, P., "Experimental Characterization of the Velocity Field of a Coaxial Jet Configuration," *Experimental Thermal and Fluid Science*, Vol. 9, No. 2, 1994, pp. 135-146.
- ³Buresti, G., Talamelli, A., and Petagna, P., "Experimental Investigation on the Turbulent Near-Field of Coaxial Jets," *Experimental Thermal and Fluid Science*, Vol. 17, No. 1-2, 1998, pp. 18-26.
- ⁴Mehta, D., "Effect of Velocity Ratio on Plane Mixing Layer Development: Influence of the Splitter Plate Wake," *Experiments in Fluids*, Vol. 10, 1991, pp. 194-204.
- ⁵Olsen, W., and Gutierrez, O., "The Effect of Nozzle Inlet Shape, Lip Thickness, and Exit Shape and Size on Subsonic Jet Noise," *AIAA Paper 73-187*, Jan. 1973.
- ⁶Olsen, W., and Karchmer, A., "Lip Noise Generated by Flow Separation from Nozzle Surfaces," *AIAA Paper 76-3*, Jan. 1976.
- ⁷Rathakrishnan, E., "Effect of Splitter Plate on Bluff Body Drag," *AIAA Journal*, Vol. 37, No. 9, 1999, pp. 135-146.

- ⁸Tamura, H., Kiya, M., and Arie, M., "Vortex Shedding from a Two-Dimensional Blunt Trailing Edge with Unequal External Free-Stream Velocities," JSME Paper 231-9, Sept. 1984.
- ⁹Bocanegra-Evans H., Allen, J.J., Wake-shear layer interaction using a soap film tunnel, Phys. Fluids 17, 091112 (2005);
- ¹⁰Wallace, D., Redekopp, L.G., Linear instability characteristics of wake-shear layers, Physics of Fluids 4, (1), January 1992.
- ¹¹Laizet, S., Lardeau, S., Lamballais, E., Direct numerical simulation of a mixing layer downstream a thick splitter plate, Phys. Fluids 22, 015104, 2010

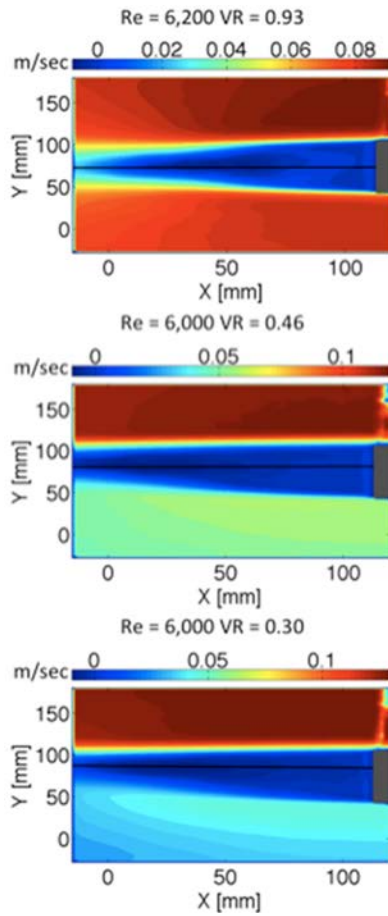


Figure 4. U_{mean} of low Re.

Top Row: $Re = 6,200$ $VR = 0.93$
 Middle Row: $Re = 6,000$ $VR = 0.46$
 Last Row: $Re = 6,000$ $VR = 0.30$

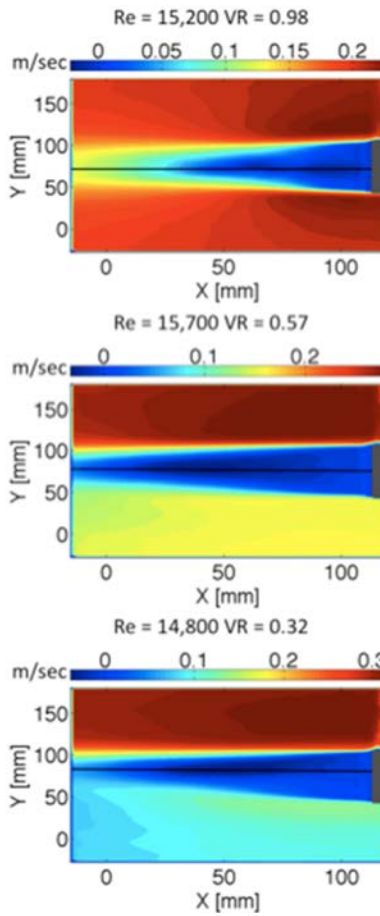


Figure 5. U_{mean} of med Re.

Top Row: $Re = 15,200$ $VR = 0.98$
 Middle Row: $Re = 15,700$ $VR = 0.57$
 Last Row: $Re = 14,800$ $VR = 0.32$

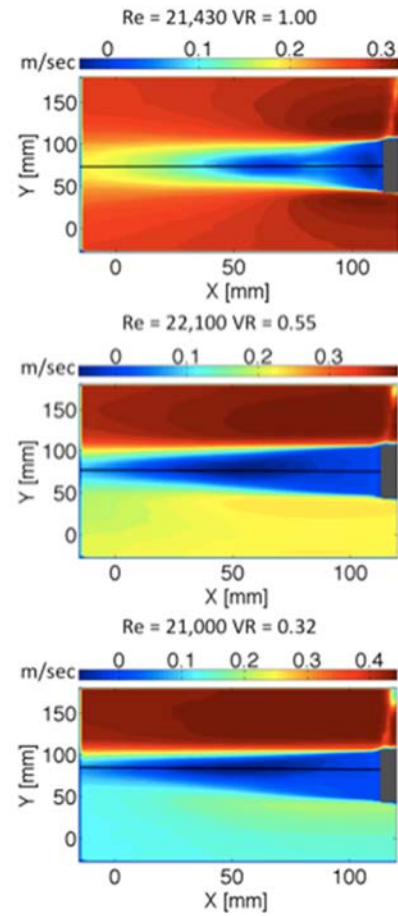


Figure 6. U_{mean} of high Re.

Top Row: $Re = 21,400$ $VR = 1.00$
 Middle Row: $Re = 22,100$ $VR = 0.55$
 Last Row: $Re = 21,000$ $VR = 0.32$

Note: The contour color levels are not uniform through all plots.

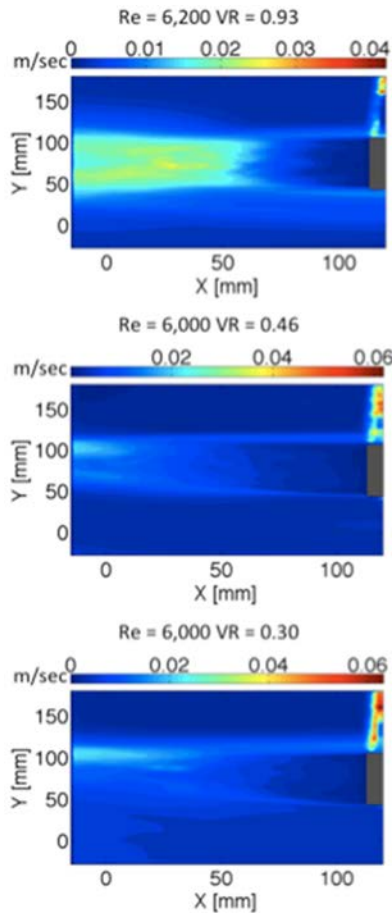


Figure 7. U_{prime} RMS of low Re.

Top Row: $Re = 6,200$ $VR = 0.93$
 Middle Row: $Re = 6,000$ $VR = 0.46$
 Last Row: $Re = 6,000$ $VR = 0.30$

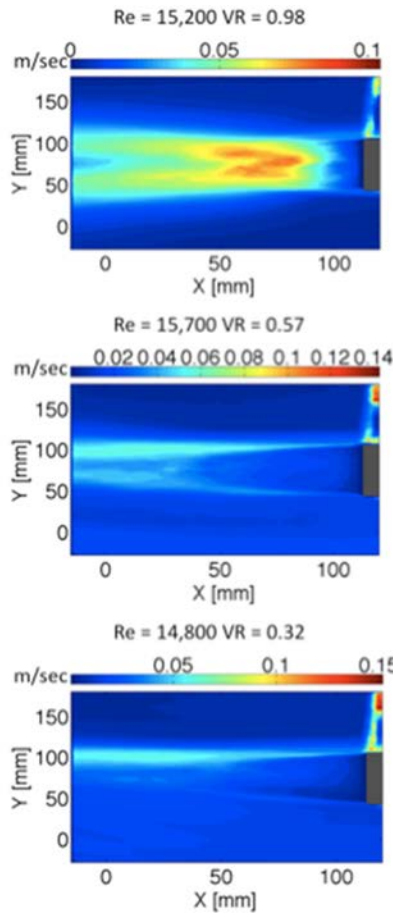


Figure 8. U_{prime} RMS of med Re.

Top Row: $Re = 15,200$ $VR = 0.98$
 Middle Row: $Re = 15,700$ $VR = 0.57$
 Last Row: $Re = 14,800$ $VR = 0.32$

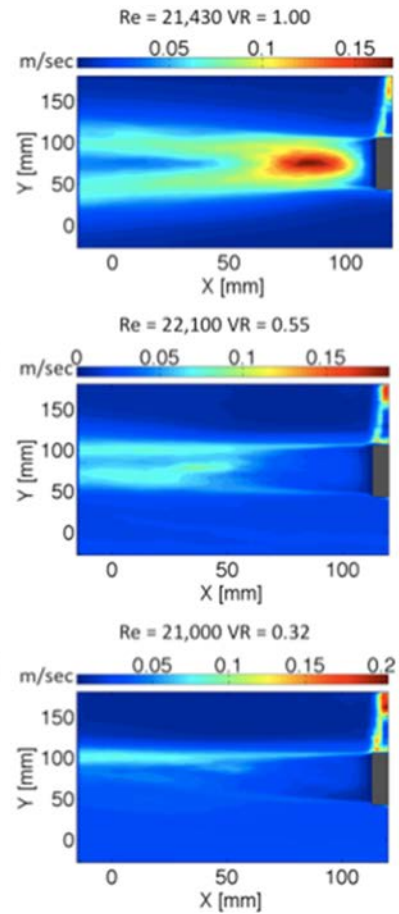


Figure 9. U_{prime} RMS of high Re.

Top Row: $Re = 21,400$ $VR = 1.00$
 Middle Row: $Re = 22,100$ $VR = 0.55$
 Last Row: $Re = 21,000$ $VR = 0.32$

Note: The contour color levels are not uniform through all plots.

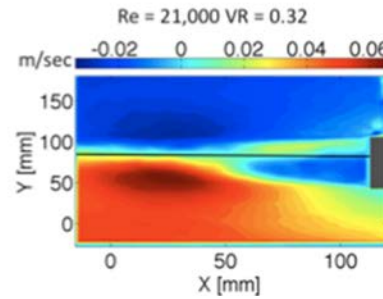
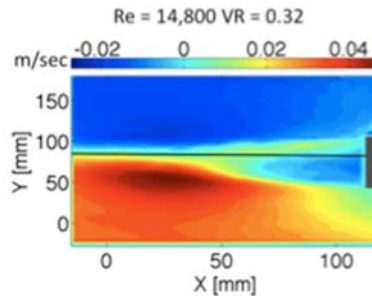
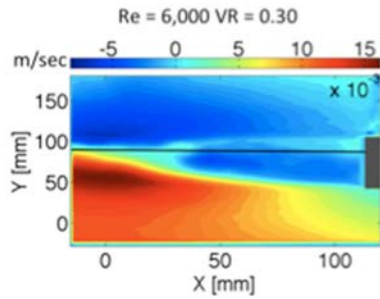
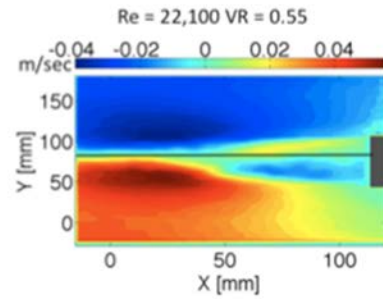
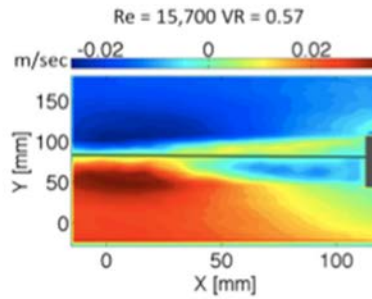
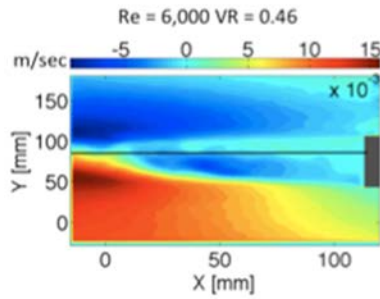
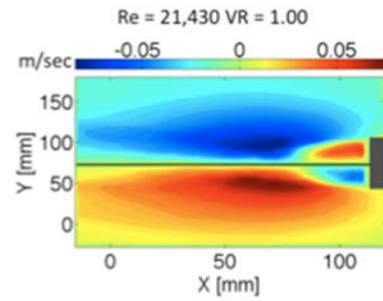
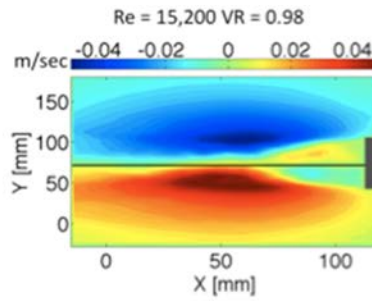
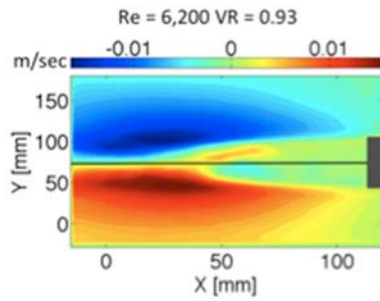


Figure 10. V_{mean} of low Re.

Top Row: $Re = 6,200$ $VR = 0.93$

Middle Row: $Re = 6,000$ $VR = 0.46$

Last Row: $Re = 6,000$ $VR = 0.30$

Figure 11. V_{mean} of med Re.

Top Row: $Re = 15,200$ $VR = 0.98$

Middle Row: $Re = 15,700$ $VR = 0.57$

Last Row: $Re = 14,800$ $VR = 0.32$

Figure 12. V_{mean} of high Re

Top Row: $Re = 21,400$ $VR = 1.00$

Middle Row: $Re = 22,100$ $VR = 0.55$

Last Row: $Re = 21,000$ $VR = 0.32$

Note: The contour color levels are not uniform through all plots.

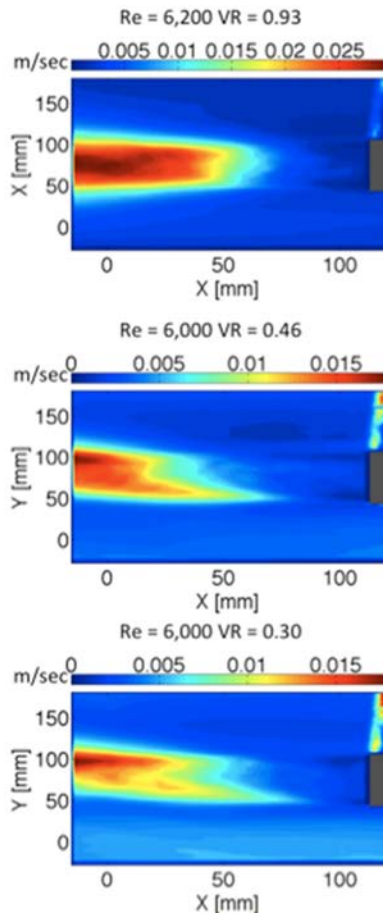


Figure 13. V_{prime} RMS of low Re.

Top Row: $Re = 6,200$ $VR = 0.93$
Middle Row: $Re = 6,000$ $VR = 0.46$
Last Row: $Re = 6,000$ $VR = 0.30$

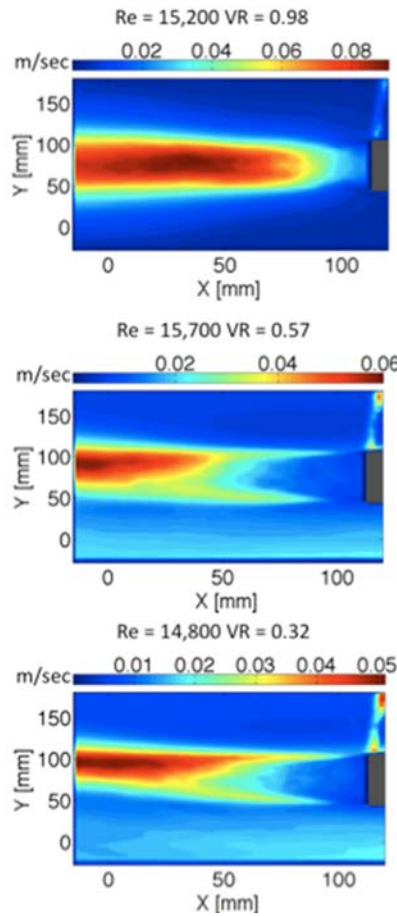


Figure 14. V_{prime} RMS of med Re.

Top Row: $Re = 15,200$ $VR = 0.98$
Middle Row: $Re = 15,700$ $VR = 0.57$
Last Row: $Re = 14,800$ $VR = 0.32$

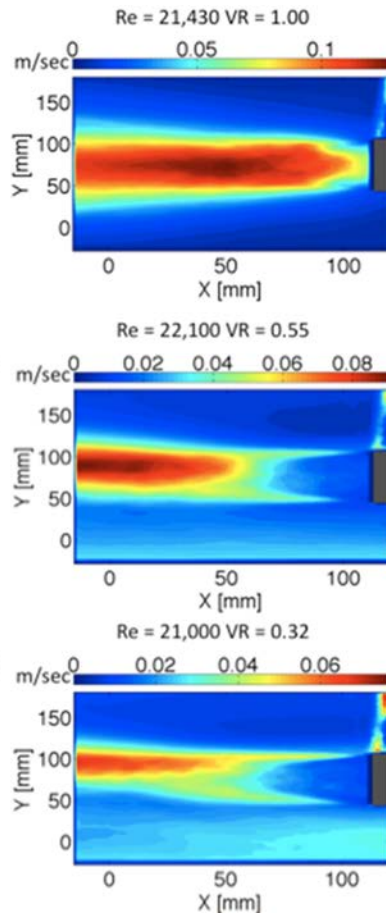


Figure 16. V_{prime} RMS of high Re.

Top Row: $Re = 21,400$ $VR = 1.00$
Middle Row: $Re = 22,100$ $VR = 0.55$
Last Row: $Re = 21,000$ $VR = 0.32$

Note: The contour color levels are not uniform through all plots.

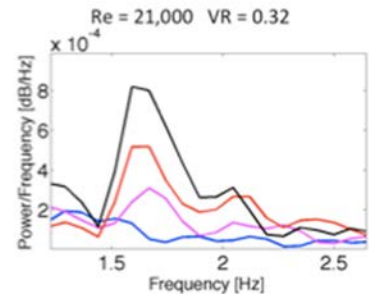
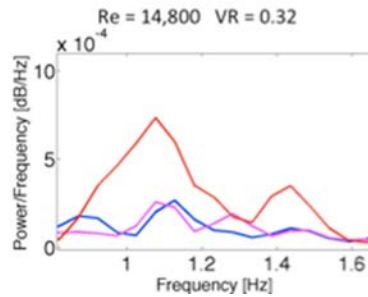
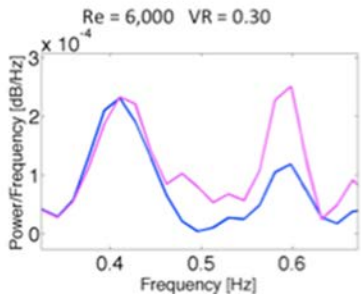
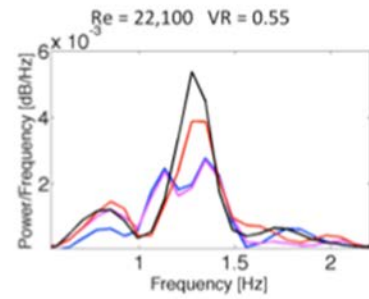
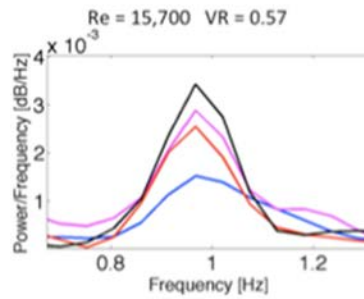
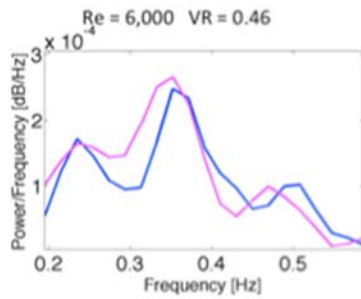
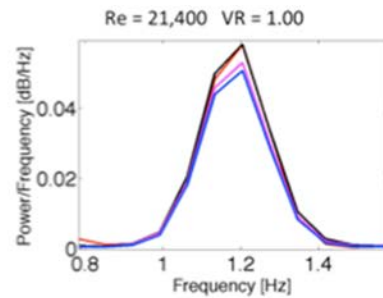
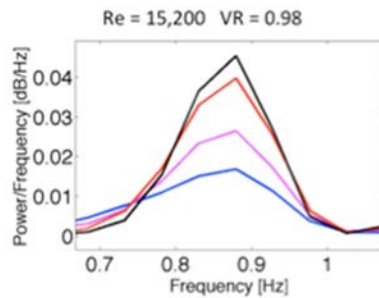
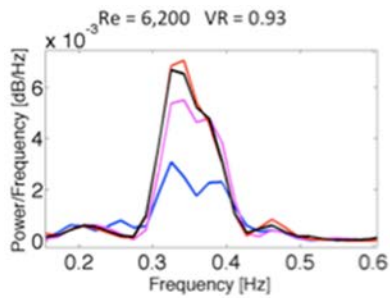


Figure 18. PSD of low Re.

Top Row: $Re = 6,200$ $VR = 0.93$

Middle Row: $Re = 6,000$ $VR = 0.46$

Last Row: $Re = 6,000$ $VR = 0.30$

Figure 19. PSD of med Re.

Top Row: $Re = 15,200$ $VR = 0.98$

Middle Row: $Re = 15,700$ $VR = 0.57$

Last Row: $Re = 14,800$ $VR = 0.32$

Figure 20. PSD of high Re.

Top Row: $Re = 21,400$ $VR = 1.00$

Middle Row: $Re = 22,100$ $VR = 0.55$

Last Row: $Re = 21,000$ $VR = 0.32$

Legend:

Blue- At the tip of the area of recirculation

Magenta- 1.0 cm from the tip of the area of recirculation

Red- 2.0 cm from the tip of the area of recirculation

Black- 3.0 cm from the tip of the area of recirculation